Aqueous Suspensions of Charged Spherical Colloids: Dependence of the Surface Charge on Ionic Strength, Acidity, and Colloid Concentration

M. N. Tamashiro,† V. B. Henriques, and M. T. Lamy

Instituto de Física, Universidade de São Paulo, Caixa Postal 66318, 05315-970 SP, São Paulo, Brazil

Received May 5, 2005. In Final Form: August 25, 2005

We theoretically investigate the dependence of the surface charge developed on charged spherical colloids upon several environmental parameters: the ionic strength of the monovalent added electrolyte, acidity (stabilized by a pH buffer solution), and colloid concentration. In the framework of the mean-field Poisson−Boltzmann spherical cell model, we include the charged colloid−microion correlations into the buffer equation, and we allow for the specific binding of ions to the ionizable groups on the colloid surface. Theoretical predictions are compared to the results obtained under the planar-symmetry Gouy−Chapman approximation and analyzed for the experimental conditions of an aqueous dispersion of the phospholipid dimyristoyl phosphatidylglycerol (DMPG). Experimental measurements of the partition ratio of an aqueous soluble cationic spin label on buffered dispersions of polyanionic unilamellar vesicles of DMPG in the presence of added monovalent salt are theoretically interpreted in terms of ion partition due to electrostatic interactions. We show that the specific binding of the probe must be admitted to explain the experimental results.

I. Introduction

Electrostatic interactions are ubiquitous in the biological realm[1−3] because virtually all biomolecules are charged in their aqueous environment. These include polynucleotides (DNA and RNA), proteins (inhomogeneously charged polypeptides), and charged membranes (lipid bilayers carrying ionizable groups).

Amphiphilic molecules, like surfactants and phospholipids, aggregate in supramolecular structures above a certain critical concentration.[4] This aggregation reduces the unfavorable contact between the solvent (usually water) and the apolar hydrocarbon tails. Whereas single-tailed surfactants form micelles with a dehydrated core, double-tailed phospholipids, because of geometric constraints, usually aggregate into bilayers. These, in turn, may form uni- or multilamellar vesicles enclosing an aqueous compartment. In both cases, the polar heads may carry ionizable groups that dissociate upon contact with water, releasing neutralizing counterions that shield the electrostatic interactions between different aggregates. Electrostatic screening may also result from the ionic dissociation of the added electrolyte in the suspension. Therefore, electrostatic effects are expected to play an important role in the formation, phase behavior, and stability of aqueous suspensions of charged phospholipid vesicles.

In particular, aqueous dispersions of dimyristoyl phosphatidylglycerol (DMPG) form polyanionic unilamellar vesicles, which constitute model systems for biological membranes because phosphatidylglycerol (PG) is the most abundant anionic phospholipid headgroup present in prokaryotic cell membranes. Because of the presence of an ionizable phosphate group, the thermostructural properties of PG lipids not only depend on the hydrocarbon chain length, but also strongly rely on the pH of the medium and on the presence of ions. DMPG, a saturated lipid with 14C atoms in each hydrophobic chain, was shown to present a rather complex thermal behavior.[5] In a range of sodium salt concentration (below ∼100 mM) and pH values (above ∼6), DMPG shows a broad gel−fluid transition region, accompanied by unusually low turbidity and high viscosity and conductivity.[6] The latter property indicates that charge dissociation may be an important effect. This transition region was named the "intermediate phase", even though it is not yet clear to what extent it can be described as a different lipid phase. Different approaches have been proposed to explain the peculiar thermotropic phase behavior of DMPG suspensions: polydispersity might play an important role,[7,8] the occurrence of rather fluid and hydrated domains, possibly high-curvature regions or perforations, coexisting with more rigid and hydrophobic bilayer patches is another possibility,[9,10] or the transition region could correspond to an extended bilayer network.[11] More evidence needs to be gathered to properly assess these different proposals. In any case, the role of explicit charge has not been analyzed in theoretical modeling,[7−11] except in ref 12. This study constitutes a more detailed investigation of the electro-

† Present address: Instituto de Física Gleb Wataghin, Universidade Estadual de Campinas, Caixa Postal 6165, 13083-970 SP, Campinas, Brazil.

(1) Lodish, H.; Berk, A.; Zipursky, S. L.; Matsudaira, P.; Baltimore, D.; Darnell, J. *Molecular Cell Biology*, 4th ed.; W. H. Freeman: New York, 2000.
(2) Alberts, B.; Johnson, A.; Lewis, J.; Raff, M.; Roberts, K.; Walter, P. *Molecular Biology of the Cell*, 4th ed.; Garland: New York, 2002.
(3) Honig, B.; Nicholls, A. *Science* **1995**, *268*, 1144.
(4) Israelachvili, J. N. *Intermolecular and Surface Forces*, 2nd ed.; Academic Press: London, 1992.
(5) Lamy-Freund, M. T.; Riske, K. A. *Chem. Phys. Lipids* **2003**, *122*, 19.
(6) Riske, K. A.; Politi, M. J.; Reed, W. F.; Lamy-Freund, M. T. *Chem. Phys. Lipids* **1997**, *89*, 31.
(7) Goldman, C.; Riske, K. A.; Lamy-Freund, M. T. *Phys. Rev. E* **1999**, *60*, 7349.
(8) Goldman, C. *J. Chem. Phys.* **2001**, *114*, 6242.
(9) Riske, K. A.; Fernandez, R. M.; Nascimento, O. R.; Bales, B. L.; Lamy-Freund, M. T. *Chem. Phys. Lipids* **2003**, *124*, 69.
(10) Riske, K. A.; Amaral, L. Q.; Döbereiner, H.-G.; Lamy, M. T. *Biophys. J.* **2004**, *86*, 3722.
(11) Schneider, M. F.; Marsh, D.; Jahn, W.; Kloesgen, B.; Heimburg, T. *Proc. Natl. Acad. Sci. U.S.A.* **1999**, *96*, 14312.

10.1021/la051211q CCC: $30.25
Published on Web 10/20/2005

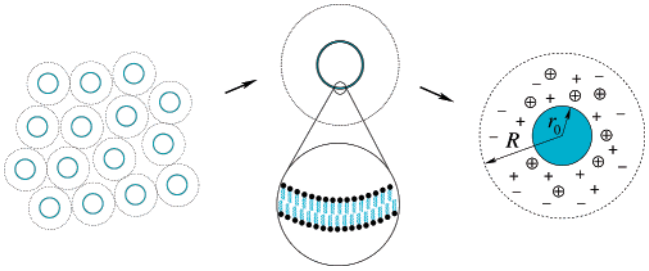

Figure 1. The cell model for a monodisperse aqueous suspension of unilamellar vesicles. The vesicle suspension is subdivided into identical spherical cells, each containing a single vesicle. The inset in the center depicts the bilayer composition, showing the ionizable polar headgroups (black circles) and the apolar hydrocarbon double tails. The rightmost sketch displays the geometry of the cell model. The spherical vesicle of total charge $-Zq$, distributed uniformly on its surface, is represented by the solid sphere of radius r_0 concentric to the spherical unitary cell of radius R. The vesicle occupies a volume fraction $\phi = (r_0/R)^3$ of the total volume of the cell $v = 4\pi R^3/3$. The mobile microscopic ions—counterions (⊕), cations (+), and anions (−)—are free to move in the spherical shell $r_0 < |\boldsymbol{r}| < R$.

static effects for a given phase (fixed form and size), with particular interest in their dependence on spherical geometry and finite lipid concentrations, which was not previously considered in ref 12.

II. The Cell Model

Our focus is on the electrostatic effects on a monodisperse aqueous suspension of charged spherical colloids. The system is treated in the framework of the cell model,[13] which has been successfully used in the description of polyelectrolyte systems.[14−16] In the spherical cell model, the suspension is subdivided into spherical cells, each containing a spherical polyion—for example, a micelle, a vesicle, or a polystyrene microsphere—and an amount of solvent and electrolyte related to the average concentrations in the system. This allows us to estimate the polyion−microion correlations, which arise from the polarization of the small mobile ions in the vicinity of the polyions: microions of opposite sign (counterions) are attracted to them, whereas like-sign microions (coions) are repelled. In this simplified framework, the mesoscopic charged polyions act as a boundary condition for the electrostatic problem. Therefore, we neglect the entropy associated with the polyion mobility and the electrostatic contributions arising from the polyion−polyion and microion−microion correlations,[17] which can be important for multivalent microions. We consider a single spherical polyion of radius r_0 that is concentric to a unitary spherical cell of total volume $v = 4\pi R^3/3$, as depicted in Figure 1. Therefore, the total volume of the cell (v) is determined by the polyion density, $v = V/N_p$, in which N_p is the total number of polyions occupying the total volume of the aqueous suspension V.

The charged spherical colloid is modeled by a solid sphere of radius $r_0 < R$ that is concentric to the unitary spherical cell. We assume a continuous (smeared) and uniform surface charge density on its surface,

$$\rho_p(\boldsymbol{r}) = -\frac{Zq}{4\pi {r_0}^2}\delta^3(|\boldsymbol{r}| - r_0), \qquad (1)$$

in which $Z \gg 1$ represents the polyion valence (number of sites actually ionized on the polyion surface), q is the proton elementary charge, and δ^3 is the tridimensional Dirac delta distribution. Without loss of generality, we consider a polyanionic (negatively charged) spherical colloid, with a surface charge that is counterbalanced by the release of Z positively charged counterions (per cell, in the external region) into the suspension. In the case of vesicles, we assume that the average concentrations of the charged species inside and outside the aqueous compartment are equal,[18] preserving the overall charge neutrality in each region separately. Therefore, there is no entrapment of microions in the hydrocarbonic hydrophobic interior (micelle cores or phospholipidic bilayer shells). With these assumptions, the analysis is simplified because the mathematical solution to the electrostatic problem in the external and internal regions is decoupled.

The electrostatic potential $\Psi(\boldsymbol{r})$ and the local volumetric charge densities $\rho_\pm(\boldsymbol{r})$ of positive and negative microions satisfy the Poisson equation

$$\nabla^2\Psi(\boldsymbol{r}) = -\nabla\cdot\boldsymbol{E}(\boldsymbol{r}) = -\frac{4\pi}{\epsilon}\{\rho_p(\boldsymbol{r}) + [\rho_+(\boldsymbol{r}) - \rho_-(\boldsymbol{r})]10^3 N_A\}, \qquad (2)$$

in which $\boldsymbol{E}(\boldsymbol{r}) = -\nabla\Psi(\boldsymbol{r})$ is the electric field at the point $\boldsymbol{r}$, the solvent is modeled as a continuous and homogeneous medium of dielectric constant ϵ, and $N_A = 6.022 \times 10^{23}$ particles/mol (Avogadro's number). We have written the volumetric charge densities in terms of molar concentrations (measured in M = mol/liter) to simplify further calculations. Henceforth, we assume that the microion densities are spherically symmetric—that is, they depend only on the distance from the center of the cell $r \equiv |\boldsymbol{r}|$—which is based on the fact that the polyion surface and the cell boundary are concentric.

For the convenience of later calculations, we have chosen to distinguish positive, X_i^+, and negative, Y_j^-, microions so that the overall local densities are given by

$$\rho_+(r) = q\sum_i [X_i^+]_r, \qquad (3)$$

$$\rho_-(r) = q\sum_{j\neq 1} [Y_j^-]_r, \qquad (4)$$

in which $[s]_r$ denotes local molar concentration of the chemical species s at a distance r from the center of the cell. The anionic species Y_1^- is reserved to denote the charged groups on the colloid surface (see eq 17) and are thus not included in eq 4.

We use a *canonical-ensemble* treatment to describe the microion concentrations in which the amount of added

(12) Riske, K. A.; Nascimento, O. R.; Peric, M.; Bales, B. L.; Lamy-Freund, M. T. *Biochim. Biophys. Acta* **1999**, *1418*, 133.
(13) Hill, T. L. *An Introduction to Statistical Thermodynamics*; Dover Publications: New York, 1986; Chapter 16.
(14) Fuoss, R. M.; Katchalsky, A.; Lifson, S. *Proc. Natl. Acad. Sci. U.S.A.* **1951**, *37*, 579.
(15) Alfrey, T.; Berg, P. W.; Morawetz, H. *J. Polym. Sci.* **1951**, *7*, 543.
(16) Marcus, R. A. *J. Chem. Phys.* **1955**, *23*, 1057.
(17) Levin, Y. *Rep. Prog. Phys.* **2002**, *65*, 1577.
(18) This assumption holds when the vesicle bilayer is impermeable to the microions, and their average concentrations $n_\pm = n_\pm^{in} = n_\pm^{out}$ are determined during the vesicle creation when a prepared aqueous buffer solution is poured onto a dehydrated phospholipidic film. In this case, the lipid bilayer isolates the intravesicular fluid from the external medium. On the other hand, if the vesicle bilayer is permeable to the charged species, then an electrochemical equilibrium is established between the two sides of the bilayer. In this case, the activities of the charged species inside and outside the vesicle are equal; $\gamma_j^{in} n_j^{in} = \gamma_j^{out} n_j^{out}$ in which γ_j^k is the activity coefficient of the species j in the region k. These conditions imply the continuity of the *local* concentrations of the charged species across the bilayer. Within the framework of the cell model, the activity coefficients taking the polyion−microion correlations into account are given by $\gamma_\pm^k = \langle e^{\mp\psi}\rangle_k^{-1}$ (see section III).

monovalent electrolyte is known a priori. This is the correct approach for the finite concentration of the colloid dispersion.[19] At the mean-field level of approximation, the local molar densities of microions are given by the Boltzmann-weighted profiles[20] for each species,

$$[X_i^+]_r = [X_i^+]_R e^{-\psi(r)}, \quad (5)$$

$$[Y_j^-]_r = [Y_j^-]_R e^{\psi(r)}, \quad (6)$$

in which $\psi(r) \equiv \beta q \Psi(r)$ is the dimensionless electrostatic potential at a distance r from the center of the cell, and $1/\beta = k_B T$ corresponds to the thermal energy at absolute temperature T. The concentrations $[X_i^+]_R$ and $[Y_j^-]_R$ are the local molar densities of the microions on the cell surface ($r = R$) where the electrostatic potential was chosen to vanish ($\psi(R) = 0$). This is an arbitrary choice, but one can generally choose any radial coordinate to gauge the zero of the electrostatic potential. The local charge densities $\rho_\pm(R)$ on the cell surface ($r = R$) can be determined by the conservation of charge in the effective volume, $v_{eff} \equiv (4\pi/3)(R^3 - r_0^3)$, which is available to the microions outside the polyion (see Figure 1),

$$\rho_\pm(R) = \frac{q n_\pm}{\langle e^{\mp\psi}\rangle}, \; n_+ \equiv [ct] + n, \; n_- \equiv n, \quad (7)$$

or, for each species,

$$[X_i^+]_R = \frac{[X_i^+]}{\langle e^{-\psi}\rangle}, \; [Y_j^-]_R = \frac{[Y_j^-]}{\langle e^{\psi}\rangle}, \quad (8)$$

in which we introduced the volumetric averages in the region that is external to the polyions,

$$\langle e^{\pm\psi}\rangle \equiv \frac{1}{v_{eff}} \int_{r_0 \le |\boldsymbol{r}| \le R} d^3\boldsymbol{r}\, e^{\pm\psi(r)}, \quad (9)$$

and the notation $n_\pm$ stands for the average molar concentrations of the charged species in the solution at equilibrium. If one assumes that dissociation is complete, both for the polyion surface and for the added monovalent electrolyte of ionic strength n, then the average molar concentration of counterions $[ct] \equiv Z/(10^3 N_A v_{eff})$ is known a priori. It should be noted that the ionic strength n does not include the counterions released by the ionization of the polyion surface.

The assumption of complete dissociation holds for aliphatic chains associated with strong acids, such as, for example, sulfonic groups when all ionizable surface sites are indeed charged. However, in most cases we need to consider the surface chemistry of the spherical colloids. Although there are several distinct chemical mechanisms leading to charge regulation, which have been investigated at different levels of approximation using different theoretical models,[21] to our knowledge, a self-consistent treatment of the bulk chemical equilibria of a buffer solution and the colloid surface chemistry has not been performed. This self-consistent treatment, which is described in the next section, is important, for example, in the determination of titration curves in concentrated colloidal suspensions. The standard titration curves obtained with the assumption of an absence of charged colloids are shifted with the addition of ionizable surfaces.

After substituting the Boltzmann-weighted profiles (eqs 5 and 6) into the Poisson equation (eq 2), the differential equation satisfied by the dimensionless electrostatic potential ψ can be cast in the form

$$\psi''(\xi) + \frac{2}{\xi}\psi'(\xi) - \kappa^2 r_0^2 \sinh[\psi(\xi) - \psi_D] = 0, \quad (10)$$

with the boundary conditions $\psi'(1) = Z l_B/r_0 = 10^3 N_A [ct] v_{eff} l_B/r_0$ and $\psi'(\phi^{-1/3}) = 0$, written in terms of the volume fraction $\phi = (r_0/R)^3$ occupied by the colloidal particles. Here, we introduce the dimensionless radial coordinate $\xi \equiv r/r_0$; the prime ($'$) in the above equation denotes differentiation with respect to the argument, and the Bjerrum length, $l_B \equiv \beta q^2/\epsilon$, measures the strength of the electrostatic interactions in the suspension, corresponding to the distance at which the electrostatic energy between two electrons equals the thermal energy $k_B T$. The inverse Debye screening length κ and the so-called Donnan potential[22] ψ_D read

$$\kappa = \sqrt{8\pi l_B 10^3 N_A}\left(\frac{n_+ n_-}{\langle e^{\psi}\rangle\langle e^{-\psi}\rangle}\right)^{1/4}, \quad (11)$$

$$\psi_D = \frac{1}{2}\ln\left(\frac{n_+\langle e^{\psi}\rangle}{n_-\langle e^{-\psi}\rangle}\right). \quad (12)$$

Here the Donnan potential ψ_D is introduced as a Lagrange multiplier conjugate to the charge-neutrality constraint.[19] Finally, the nonlinear second-order differential (eq 10) can be solved numerically by recasting the two-point boundary value problem into a one-point boundary value problem[23] by assigning an a priori value for the Donnan potential ψ_D.

For the sake of clarity, we compare our approach with the more common treatment, which is adequate for very dilute systems, in which the polyion suspension may be considered to be in electrochemical equilibrium with an infinite electrolyte reservoir of bulk molar density c_b. In this *semigrand canonical* approach, the inverse Debye screening length reduces to the standard definition $\kappa = \sqrt{8\pi l_B 10^3 N_A c_b}$, and the Donnan potential is related to the difference Δp between the osmotic pressure in the colloidal suspension and that in the infinite reservoir,[16,22]

$$10^{-3} N_A^{-1} \beta \Delta p = \frac{1}{q}[\rho_+(R) + \rho_-(R)] - 2c_b = 4c_b \sinh^2\left[\frac{1}{2}\psi(\phi^{-1/3}) - \frac{1}{2}\psi_D\right]. \quad (13)$$

There is a simple relation involving the average molar concentrations of the charged species in the colloidal suspension $n_\pm$, the average molar concentration of counterions [ct], and bulk molar concentration of the infinite reservoir c_b,

$$n_\pm = \frac{1}{2}\sqrt{[ct]^2 + (2c_b)^2\langle e^{\psi}\rangle\langle e^{-\psi}\rangle} \pm \frac{1}{2}[ct]. \quad (14)$$

(19) Tamashiro, M. N.; Schiessel, H. EPAPS Document E-JCPSA6-119-516326. http://www.aip.org/pubservs/epaps.html. Complement to *J. Chem. Phys.* **2003**, *119*, 1855.

(20) Deserno, M.; Holm, C. Cell model and Poisson−Boltzmann theory: a brief introduction. In *Proceedings of the NATO Advanced Study Institute on Electrostatic Effects in Soft Matter and Biophysics*; Holm, C., Kékicheff, P., Podgornik, R., Eds.; Kluwer: Dordrecht, The Netherlands, 2001; pp 27.

(21) Hunter, R. J. *Zeta potential in colloid science: principles and applications*, 2nd printing; Academic Press: London, 1986.

(22) Tamashiro, M. N.; Levin, Y.; Barbosa, M. C. *Eur. Phys. J. B* **1998**, *1*, 337.

These indeed yield $n_\pm = c_b$ in the limit of the infinite dilution of polyions when $[ct]/c_b \to 0$ and $\langle e^{\pm\psi}\rangle \to e^{\pm\psi(R)}$. Using the above relations between the canonical and semigrand canonical treatments, the Poisson−Boltzmann equation can be written in its standard form,

$$\nabla^2\psi = \kappa^2 \sinh \psi, \tag{15}$$

with the boundary conditions $\hat{\boldsymbol{r}}\cdot\nabla\psi|_{r=r_0} = Zl_B/r_0^2$ and $\hat{\boldsymbol{r}}\cdot\nabla\psi|_{r\to\infty} = 0$. Note that, in the standard form of the Poisson−Boltzmann equation, the gauge is chosen such that the Donnan potential vanishes ($\psi_D \equiv 0$) which *does not* correspond to the gauge in which the electrostatic potential at the cell surface or in the infinite reservoir vanishes. Clearly, in the semigrand canonical treatment, the Debye screening length depends only on the bulk molar concentration (c_b) of the infinite reservoir. We note, therefore, that, unlike the above canonical treatment (cf. eq 11), the semigrand canonical treatment should not include the average concentration of counterions [ct] in the ionic strength to compute κ.

III. Surface Charge Regulation

The Poisson−Boltzmann eq 10 can be used to obtain the electrostatic potential if the number Z of actually ionized sites on the colloid surface is known a priori. However, our interest lies in analyzing the case in which the dissociation on the colloid surface is only partial. Note that, in this case, the ionic strength n and the counterion molar density [ct] appearing in eq 7 are no longer a priori-known quantities, but rather must be calculated from the surface chemistry of the spherical colloids. Thus, we rewrite eq 7 as

$$\rho_\pm(R) = \frac{q[c_\pm]}{\langle e^{\mp\psi}\rangle}, \quad [c_+] \equiv [ct] + [c_-], \tag{16}$$

in which the bracket notation $[c_\pm]$ for the equilibrium molar concentrations of the charged species indicates that they are unknown a priori and must be found from charge regulation. We use the notation $n_{X_iY_j}$ for initial (known a priori) molar concentrations and $[X_i^+]$, $[Y_j^-]$ for unknown molar concentrations, which must be determined from charge-neutrality and mass-conservation conditions to be derived below. For example, if the neutral monovalent electrolyte X_iY_j of molar concentration $n_{X_iY_j}$ undergoes complete ionization in water ($X_iY_j \to X_i^+ + Y_j^-$) and there is no association of the conjugated charged species X_i^+ and Y_j^- to the colloid surface, then their equilibrium molar concentrations, denoted by $[X_i^+]$ and $[Y_j^-]$, are known a priori and simply given by $n_{X_iY_j} = [X_i^+] = [Y_j^-]$. However, for the general case of partial ionization in water and/or association to the colloid surface, the equilibrium molar concentrations have to be determined by the conditions of chemical equilibrium.

Henceforth, we consider, for simplicity, only ionogenic surfaces containing monovalent weak acidic groups in a salt form, $\bar{J}^+J^-_{surf}$, which can partially dissociate to yield an aqueous soluble cationic counterion $\bar{J}^+$ in the solution, leaving negatively charged sites J^-_{surf} on the colloid surface. Here the subscript "surf" stands for chemical species on the colloid surface, and the bar notation on the free cationic species $\bar{J}^+$ indicates that it is conjugated to the anionic species J^-_{surf}, which is attached to the colloid surface. Furthermore, we allow for the specific binding of ions to the ionizable groups on the colloid surface. For negatively charged surfaces, the chemical binding of anions is electrostatically unfavorable and can be neglected, but the specific adsorption of the cations to the anionic surface groups must be included in the model. Therefore, the surface charge density developed on the spherical polyanions may depend on the local volumetric molar densities at the colloid surface $[X_i^+]_{r_0}$ of the protons (local surface pH) or any other positive microions present in the system. Like the protons (H^+) and the strict counterions ($\bar{J}^+$) released by the dissociation of the surface groups on the colloids, all positively charged species may act as potential determining ions; that is, the polyion surface charge is determined by the specific binding of the cationic species X_i^+ to the acidic surface groups J^-_{surf}.

A. Dissociation Constants. To establish the conditions of chemical equilibrium, one has to consider all of the chemical reactions that occur in the colloidal suspension. Let us first consider the partial dissociation of the weak acidic groups on the colloid surface, which gives origin to the conjugated cationic/anionic pair (X_1^+, Y_1^-),

$$\bar{J}J_{surf} \rightleftharpoons \bar{J}^+ + J^-_{surf}, \; X_1^+ \equiv \bar{J}^+, \; Y_1^- \equiv J^-_{surf}. \tag{17}$$

To stabilize the proton molar concentration $[H^+]$ of the solution—ideally to keep it constant—a buffer solution is employed, which consists of a weak acid, HA, characterized by the dissociation equilibrium constant K_A and an initial total molar concentration n_{HA}, which is adjusted by the addition of strong bases of molar concentrations n_{X_iOH} ($i \neq 2$). These solutes are immersed in water, characterized by its ionic product K_W. The relevant chemical reactions for the buffer solution are the water autoprotolysis, the partial ionization of the weak acid HA, and the complete dissociation of the strong bases X_iOH,

$$H_2O \rightleftharpoons H^+ + OH^-, \; X_2^+ \equiv H^+, \; Y_2^- \equiv OH^-, \tag{18}$$

$$HA \rightleftharpoons H^+ + A^-, \; Y_3^- \equiv A^-, \tag{19}$$

$$X_iOH \to X_i^+ + OH^-, \text{ for } i \neq 2. \tag{20}$$

It should be noted that the indexes (i, j) of the charged species (X_i^+, Y_j^-) label the chemical components and not the chemical reactions. According to the above notation, for example, the weak acid HA is represented thus by X_2Y_3. In Appendix A we present the standard treatment of a buffer solution as a homogeneous electrolyte neglecting activity coefficients. In the presence of charged colloids, however, the buffer solution must be treated self-consistently in the framework of the Poisson−Boltzmann spherical cell model. To be consistent with the inclusion of the polyion−microion correlations in the cell model, it is necessary to use the strict definition of the dissociation equilibrium constants in terms of the activities,

$$K_W \equiv a_{H^+}\, a_{OH^-} = \gamma^2[H^+][OH^-], \tag{21}$$

$$K_A \equiv \frac{a_{H^+}\, a_{A^-}}{a_{HA}} = \gamma^2\frac{[H^+][A^-]}{[HA]} = \gamma^2\frac{[H^+][A^-]}{n_{HA} - [A^-]}, \tag{22}$$

in which the activity coefficient of the undissociated weak acid $\gamma_{HA} = 1$, $\gamma = \sqrt{\gamma_+\gamma_-}$ is the mean activity coefficient (for monovalent microions), and $\gamma_\pm \equiv \langle e^{\mp\psi}\rangle^{-1}$ is the activity coefficient for the positive and negative microions. These are based on the definition of the activities of the charged

(23) Trizac, E.; Bocquet, L.; Aubouy, M.; von Grünberg, H. H. *Langmuir* **2003**, *19*, 4027.

species, $a_j = e^{\beta\mu_j}/\Lambda_j^3 = 10^3 N_A \gamma_j n_j$, in which $\beta\mu_j = \ln(10^3 N_A n_j \Lambda_j^3) - \ln\langle e^{\mp\psi}\rangle$ is the corresponding electrochemical potential for the positive/negative microions, in unities of $k_B T$, and Λ_j is the associated thermal de Broglie wavelength. If the contribution of the microion−microion and polyion−polyion correlations to the activity coefficients $\gamma_\pm$ can be neglected, then the equilibrium constants K_W and K_A, as given by eqs 21 and 22, should coincide with their values in a colloid-free buffer aqueous solution.

Monovalent salts (assumed to be strong) may be added to the system and undergo complete ionization in the aqueous suspension,

$$X_i Y_j \rightarrow X_i^+ + Y_j^-, \text{ for } i \neq 2 \text{ and } j \geq 4. \qquad (23)$$

Finally, in addition to the partial surface charge dissociation involving the strict counterion $\bar{J}^+$ (eq 17), reversible chemical binding of cations X_i^+ ($i \geq 2$) to the weak acidic surface groups J^-_{surf} may also take place on the colloid surface,

$$X_i J_{surf} \rightleftharpoons X_i^+ + J^-_{surf}, \text{ for } i \neq 1. \qquad (24)$$

The partial dissociation of the surface charged groups J^-_{surf} may be described in terms of the association constants K_i (measured in M^{-1} = liter/mol) of the acidic groups J^-_{surf} on the polyion surface to the generic cationic species X_i^+,

$$K_i \equiv \frac{a_{X_i J_{surf}}}{a_{J^-_{surf}} [X_i^+]_{r_0}}, \qquad (25)$$

in which X_i^+ stands for protons or any other cations, including the released strict counterions $X_1^+ = \bar{J}^+$, the notation $[\cdots]_{r_0}$ represents a volumetric molar concentration at the polyion surface ($r = r_0$), and a_j denotes the chemical activity of the species j. In a mean-field (ideal-gas) approximation, the associated surface activities are given by their surface molar densities, yielding

$$K_i = \frac{[X_i J_{surf}]}{[J^-_{surf}][X_i^+]_{r_0}} = \frac{[X_i J_{surf}]}{[ct][X_i^+]_{r_0}}, \qquad (26)$$

which results from the charge-neutrality constraint because $[J^-_{surf}] = [ct]$, and [ct] is the equilibrium molar concentration of counterions (now unknown a priori), which has to be determined by the conditions of chemical equilibrium.

The local molar concentrations of the cationic species at the polyion surface $[X_i^+]_{r_0}$ that appear in eq 26 can then be determined by taking into account their partial contributions to the average concentration of positive microions at equilibrium from eqs 3 and 5,

$$[X_i^+]_{r_0} = [X_i^+] \frac{e^{-\psi_0}}{\langle e^{-\psi}\rangle}, \qquad (27)$$

in which $\psi_0 \equiv \psi(\xi = 1)$ is the dimensionless electrostatic potential at the polyion surface, the value of which depends on the choice of the gauge. Thus, eq 26 can be rewritten as

$$K_i = \frac{[X_i J_{surf}]}{[J^-_{surf}][X_i^+]_{r_0}} = \frac{[X_i J_{surf}]}{[ct][X_i^+]\, e^{-\psi_0}/\langle e^{-\psi}\rangle}. \qquad (28)$$

B. Charge Neutrality and Mass Conservation. Charge neutrality and mass conservation allow us to write some additional equations to characterize the chemical equilibrium.

The global concentration of surface-forming acidic salt, $n_{\bar{J}J}$, is known from experimental conditions,[24] so summing up dissociating and associated groups on the colloid surface leads to a mass-conservation equation,

$$n_{\bar{J}J} = [J^-_{surf}] + \sum_i [X_i J_{surf}] = [ct]\left(1 + \sum_i K_i [X_i^+] \frac{e^{-\psi_0}}{\langle e^{-\psi}\rangle}\right), \qquad (29)$$

in which the expression on the right-hand side is based on eq 28. Note that the sum in eq 29 includes the strict-counterion contribution ($i = 1$).

The equilibrium concentration of the strict counterions $[\bar{J}^+]$, apart from the colloid surface partial ionization $n_{\bar{J}J} - [\bar{J}J_{surf}]$, may have contributions from added strong salts and/or strong base, denoted by $\bar{J}Y_j$ ($j \neq 1$), which undergo complete dissociation in the aqueous suspension ($\bar{J}Y_j \rightarrow \bar{J}^+ + Y_j^-$). Its mass conservation is thus written as

$$[\bar{J}^+] = n_{\bar{J}J} - [\bar{J}J_{surf}] + \sum_{j\neq 1} n_{\bar{J}Y_j} = [ct]\left(1 + \sum_{i\neq 1} K_i [X_i^+] \frac{e^{-\psi_0}}{\langle e^{-\psi}\rangle}\right) + \sum_{j\neq 1} n_{\bar{J}Y_j}. \qquad (30)$$

The expression on the right is based on eq 29 and the fact that $[\bar{J}J_{surf}] = [X_1 J_{surf}] = K_1 [ct][X_1^+]_{r_0}$ (from eq 26). It is noteworthy that the sums in eq 30 do not include the contributions from the strict counterions ($i = 1$) nor those from the acidic surface groups ($j = 1$).

Mass conservation of the X_i^+ counterions ($i \geq 3$)—thus excluding strict counterions ($i = 1$) and protons ($i = 2$)—reads

$$[X_i^+] + [X_i J_{surf}] = \sum_{j\neq 1} n_{X_i Y_j}, \text{ for } i \geq 3, \qquad (31)$$

because the total concentration of a particular cationic species X_i^+ can be split into ions in solution plus ions chemically bound to the colloid surface. The latter must balance the total concentrations of the fully dissociating added salts and bases that involve that particular species. By using eq 28 we obtain

$$[X_i^+] = \frac{\sum_{j\neq 1} n_{X_i Y_j}}{1 + K_i [ct] e^{-\psi_0}/\langle e^{-\psi}\rangle}, \text{ for } i \geq 3. \qquad (32)$$

Now we may write mass-conservation equations for the positive and negative ions in solution,

$$[c_+] = \sum_i [X_i^+] = [\bar{J}^+] + [H^+] + \sum_{i\geq 3} [X_i^+], \qquad (33)$$

$$[c_-] = \sum_{j\neq 1} [Y_j^-] = [OH^-] + [A^-] + \sum_{i\neq 2} \sum_{j\geq 4} n_{X_i Y_j}. \qquad (34)$$

From the mass-conservation conditions above (eqs 29, 30, and 32−34), we may now write two equations: (1) one

equation for the concentration of surface-forming acidic salt,

$$n_{\bar{J}J} = [\mathrm{ct}]\frac{\mathrm{e}^{-\psi_0}}{\langle \mathrm{e}^{-\psi}\rangle}\Bigg[K_{\bar{J}}\sum_{j\neq 1} n_{\bar{J}Y_j} + (\mathrm{e}^{\psi_0}\langle \mathrm{e}^{-\psi}\rangle + K_{\bar{J}}[\mathrm{ct}])\Bigg(1 + \sum_{i\neq 1} K_i[X_i^+]\frac{\mathrm{e}^{-\psi_0}}{\langle \mathrm{e}^{-\psi}\rangle}\Bigg)\Bigg]$$

$$= [\mathrm{ct}]\frac{\mathrm{e}^{-\psi_0}}{\langle \mathrm{e}^{-\psi}\rangle}\Bigg[K_{\bar{J}}\sum_{j\neq 1} n_{\bar{J}Y_j} + (\mathrm{e}^{\psi_0}\langle \mathrm{e}^{-\psi}\rangle + K_{\bar{J}}[\mathrm{ct}])\Bigg(1 + K_{\mathrm{H}}[\mathrm{H}^+]\frac{\mathrm{e}^{-\psi_0}}{\langle \mathrm{e}^{-\psi}\rangle} + \sum_{i\geq 3}\frac{K_i\sum_{j\neq 1} n_{X_iY_j}}{\mathrm{e}^{\psi_0}\langle \mathrm{e}^{-\psi}\rangle + K_i[\mathrm{ct}]}\Bigg)\Bigg], \quad (35)$$

in which $K_{\bar{J}} = K_1$, $K_{\mathrm{H}} = K_2$, and the second equality is based on eq 32 and (2) an equation for the equilibrium molar concentration of counterions, $[\mathrm{ct}] = [c_+] - [c_-]$, using eq 21 for $[\mathrm{OH}^-]$, 22 for $[\mathrm{A}^-]$, and 32 for $[X_i^+]$,

$$[\mathrm{ct}] = [\bar{J}^+] + [\mathrm{H}^+] - \frac{K_{\mathrm{W}}}{\gamma^2[\mathrm{H}^+]} - \frac{n_{\mathrm{HA}}}{1 + \gamma^2[\mathrm{H}^+]/K_{\mathrm{A}}} - \sum_{j\geq 4} n_{\bar{J}Y_j} + \sum_{i\geq 3} n_{X_i\mathrm{OH}} - [\mathrm{ct}]\sum_{i\geq 3} K_i[X_i^+]\frac{\mathrm{e}^{-\psi_0}}{\langle \mathrm{e}^{-\psi}\rangle}$$

$$= [\mathrm{H}^+] - \frac{K_{\mathrm{W}}}{\gamma^2[\mathrm{H}^+]} - \frac{n_{\mathrm{HA}}}{1 + \gamma^2[\mathrm{H}^+]/K_{\mathrm{A}}} + \sum_{i\neq 2} n_{X_i\mathrm{OH}} + [\mathrm{ct}]\Bigg(1 + K_{\mathrm{H}}[\mathrm{H}^+]\frac{\mathrm{e}^{-\psi_0}}{\langle \mathrm{e}^{-\psi}\rangle}\Bigg), \quad (36)$$

in which the second equality is obtained by using eq 30 for $[\bar{J}^+]$. The latter equation can be rewritten as

$$K_{\mathrm{W}}K_{\mathrm{A}} = (K_{\mathrm{A}} + \gamma^2[\mathrm{H}^+])\gamma^2[\mathrm{H}^+]^2K_{\mathrm{H}}[\mathrm{ct}]\frac{\mathrm{e}^{-\psi_0}}{\langle \mathrm{e}^{-\psi}\rangle} + \gamma^4[\mathrm{H}^+]^3 + (K_{\mathrm{A}} + \gamma^2\sum_{i\neq 2} n_{X_i\mathrm{OH}})\gamma^2[\mathrm{H}^+]^2 - \{K_{\mathrm{W}} + K_{\mathrm{A}}(n_{\mathrm{HA}} - \sum_{i\neq 2} n_{X_i\mathrm{OH}})\}\gamma^2[\mathrm{H}^+]. \quad (37)$$

Equations 35 and 37 constitute a set of equations that must be solved for the equilibrium molar concentration of counterions [ct] and the equilibrium molar concentration of protons $[\mathrm{H}^+]$. This set can be solved, provided the association constants $\{K_1, K_2, \cdots\}$ for cationic association to the colloid surface are established from independent experimental measurements.

Equation 37 may be compared to the colloid-free buffer eq A3, which neglects activity coefficients, derived in Appendix A. Unlike the colloid-free case, it is not possible to simplify the coupled system in the limit $\sum_{i\neq 2} n_{X_i\mathrm{OH}} \gg [\mathrm{H}^+]$ and $\sum_{i\neq 2} n_{X_i\mathrm{OH}} \gg [\mathrm{OH}^-]$ because of the coupling introduced by the average counterion concentration at equilibrium [ct].

(24) For unilamellar phospholipid vesicles, for example, $n_{\bar{J}J} = Z_{\max}/(10^3 N_{\mathrm{A}} v_{\mathrm{eff}})$, in which the bare polyion valence $Z_{\max}$ represents the total number of polar headgroups in the outer bilayer leaflet, which is known a priori for a given vesicle size and area per lipid headgroup.

To determine the surface electrostatic potential of the colloidal particles, $\Psi_0 = \psi_0/(\beta q)$, in the gauge where the potential at the cell boundary vanishes, $\Psi(R) = 0$, one has to solve the Poisson−Boltzmann-like eq 10 simultaneously and self-consistently with eqs 35 and 37, with the molar density of coions given by

$$[c_-] = [c_+] - [\mathrm{ct}] = \sum_{i\neq 2}\sum_{j\neq 1} n_{X_iY_j} + [\mathrm{H}^+]\Bigg(1 + K_{\mathrm{H}}[\mathrm{ct}]\frac{\mathrm{e}^{-\psi_0}}{\langle \mathrm{e}^{-\psi}\rangle}\Bigg), \quad (38)$$

and eqs 11 and 12 are evaluated with the replacements $n_\pm \rightarrow [c_\pm]$.

C. Partition Ratios. Now, it may be of interest to find the partition ratios of the microions. In general, one may distinguish three populations: chemically bound (dehydrated, specifically adsorbed) microions on the colloid surface, physically bound (hydrated, electrostatically associated) ions near the polyion surface and free ions away from the colloid surface. To describe the two latter populations, we need to find the ionic distribution as a function of the distance from the charged surface. The integrated charge of positive microions (excluding those specifically adsorbed) from the polyion surface at $r = r_0$ to the position $\bar{r} = \bar{\xi} r_0$ reads

$$Q_+(\bar{r}) = 4\pi {r_0}^3 \rho_+(R)\int_1^{\bar{\xi}} \mathrm{d}\xi\, \xi^2\, \mathrm{e}^{-\psi(\xi)}. \quad (39)$$

The integrand of the latter expression, $\xi^2\, \mathrm{e}^{-\psi(\xi)}$, can be interpreted as a probability density to find a positive microion at the position r and has a minimum at $\bar{\xi}$ that satisfies the relation $\psi'(\bar{\xi}) = 2/\bar{\xi}$ (see Figure 2). Therefore, we might use the distance $\bar{r}$ as a cutoff to classify the positive ions: cations located at $r < \bar{r}$ would be electrostatically associated to the charged colloid, whereas those located at $r > \bar{r}$ would be free.

This leads to the partition ratio P_i of the cationic species X_i^+, defined as the fraction of ions that are either specifically adsorbed onto or electrostatically associated in the vicinity of the colloid surface, compared to their total number,

$$P_i = \frac{1}{v_{\mathrm{eff}}\sum_{j\neq 1} n_{X_iY_j}}\Bigg(v_{\mathrm{eff}}[X_iJ_{\mathrm{surf}}] + \frac{4\pi {r_0}^3}{\langle \mathrm{e}^{-\psi}\rangle}[X_i^+]\int_1^{\bar{\xi}} \mathrm{d}\xi\, \xi^2 \mathrm{e}^{-\psi(\xi)}\Bigg)$$

$$= \frac{[X_i^+]}{v_{\mathrm{eff}}\,\mathrm{e}^{\psi_0}\langle \mathrm{e}^{-\psi}\rangle\sum_{j\neq 1} n_{X_iY_j}}(v_{\mathrm{eff}}K_i[c^+] + 4\pi {r_0}^3 \mathrm{e}^{\psi_0}\int_1^{\bar{\xi}} \mathrm{d}\xi\, \xi^2 \mathrm{e}^{-\psi(\xi)}). \quad (40)$$

IV. Results and Comparison with Experiments

We now analyze and compare our theoretical results with several experimental measurements and previous calculations for aqueous DMPG suspensions.[12]

The general model for charge regulation, outlined in the preceding section, is applied for the system under study when the negative surface charge density $\sigma_{\mathrm{PG}^-} = v_{\mathrm{eff}}[J_{\mathrm{surf}}^-]/(4\pi {r_0}^2)$ developed on the DMPG vesicle—or alternatively, the associated equilibrium average counterion density $[\mathrm{ct}] = Z/(10^3 N_{\mathrm{A}} v_{\mathrm{eff}})$—depends on the local concentrations of positive microions at the vesicle surface.

From the experimental side, the aqueous soluble cationic spin label $\mathrm{dCAT1}^+$ (in the form of the iodide salt 4-trimethylammonium-2,2,6,6-tetramethyl-piperidine-d_{17}-1-oxyl iodide), of known initial concentration n_{dCAT1I}, can be

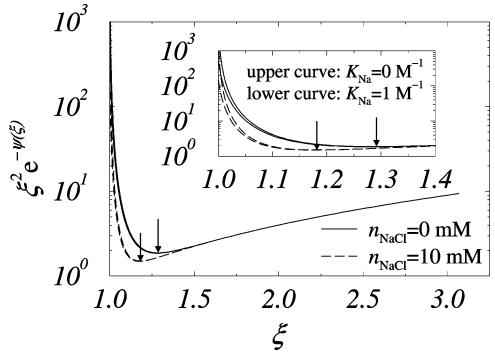

Figure 2. Linear-log plot of the probability function $\xi^2 e^{-\psi(\xi)}$ as a function of ξ, showing the minima at $\xi = \bar{\xi}$, which are denoted by the arrows. Note the steep increase in the electrostatic potential close to the vesicle surface. In the gauge chosen, the electrostatic potential at the cell boundary vanishes $\psi(\xi = \phi^{-1/3}) = 0$. The four profiles were obtained with different combinations of the ionic strength and the sodium association constant to the phosphate surface groups K_{Na}. Pairs of curves with the same ionic strength differ only in the vicinity of the vesicle surface, as shown in the inset.

used to monitor the negatively charged DMPG vesicle surface. The nitroxide group incorporated into this probe yields different electron spin resonance spectra according to its microenvironment. The experimentally measured composite spectra could be split into two components[12] that differ in the mobility of the spin labels. These distinct components can be attributed to regions where the strength of the electrostatic field differs drastically. Close to the charged vesicle surface, the cationic probes are strongly attracted to the oppositely charged phosphate groups, whereas, in the bulk, the Coulomb interactions are much weaker. Label partition between the charged lipid surface and the aqueous medium could then be used to infer the electrostatic potential at the vesicle surface.

In a previous study,[12] this task was undertaken under three simple assumptions:

(1) no specific binding of the probe to the phosphate surface groups ($K_{dCAT1} = 0$ M^{-1});

(2) partition was associated with a two-population model of physically bound and free probes under a common chemical potential. To develop calculations for the surface potential ψ_0, an arbitrary thickness for the region of bound probes had to be adopted; and

(3) the results for the surface potential ψ_0 that were obtained from assumptions (1) and (2) were compared to Poisson−Boltzmann calculations based on planar geometry (the Gouy−Chapman model).

Here, we propose to remove the arbitrariness in the definition of the partition regions. Also, we check on the role of geometry in the calculation of the surface potential under the circumstances of this particular experiment as well as on the consistency of hypothesizing null probe binding with experimental findings.

In the first subsection (IV-A), we compare the surface electrostatic potentials obtained from theory under the spherical and planar geometries, under the experimental conditions, and on the assumption of no specific binding of the probe to the phosphate surface groups.

In the second subsection (IV-B), we compare the experimental results for the spin-label partitioning with our theoretical predictions, showing that they cannot be reconciled unless some specific binding of the probe is assumed.

A. Surface Electrostatic Potential. First, we present our theoretical predictions of the surface electrostatic potential of spherical vesicles for the range of parameters relevant to the experiments performed on aqueous DMPG suspensions.[12]

The general equations of section III must be applied for the single acidic surface phosphate group $Y_1^- = PG_{surf}^-$ on DMPG vesicles. Because the sodium salt of DMPG was used in the experiments, the sodium cation represents the strict counterion $X_1^+ = Na^+$. The pH of the suspension was adjusted with the strong base X_1OH = NaOH, and the ionic strength was varied by the addition of the monovalent salt X_1Y_4 = NaCl. The aqueous soluble cationic spin label represents an added monovalent salt, X_3Y_5 = dCAT1I, which ionizes neither into protons nor strict counterions (sodium cations).

Aside from the deprotonated charged groups (PG_{surf}^-), three different neutral species of phosphate groups on the vesicle surface must be considered: protonated (HPG_{surf}) groups and those chemically bound to either sodium cations ($NaPG_{surf}$) or cationic spin labels ($dCAT1PG_{surf}$). Because the sodium salt of the phospholipid DMPG was used in the experiments, the average concentration of sodium cations [Na^+] can be determined by the sodium mass conservation (eq 30),

$$[Na^+] = n_{NaOH} + n_{NaCl} + [ct](1 + K_H[H^+]_{r_0} + K_{dCAT1}[dCAT1^+]_{r_0}). \quad (41)$$

The average proton concentration [H^+] is determined by the charge-neutrality constraint, allowing one to obtain a coupled system that is satisfied by the equilibrium values of the counterion density [ct] and the proton concentration [H^+] (eqs 35 and 37),

$$n_{NaPG} = [ct]\frac{e^{-\psi_0}}{\langle e^{-\psi}\rangle}\left[(n_{NaOH} + n_{NaCl})K_{Na} + (e^{\psi_0}\langle e^{-\psi}\rangle + K_{Na}[ct])\left(1 + K_H[H^+]\frac{e^{-\psi_0}}{\langle e^{-\psi}\rangle} + \frac{n_{dCAT1I}K_{dCAT1}}{e^{\psi_0}\langle e^{-\psi}\rangle + K_{dCAT1}[ct]}\right)\right], \quad (42)$$

$$K_W K_A = (K_A + \gamma^2[H^+])\gamma^2[H^+]^2 K_H[ct]\frac{e^{-\psi_0}}{\langle e^{-\psi}\rangle} + \gamma^4[H^+]^3 + (K_A + \gamma^2 n_{NaOH})\gamma^2[H^+]^2 - \{K_W + K_A(n_{HA} - n_{NaOH})\}\gamma^2[H^+]. \quad (43)$$

To obtain the surface electrostatic potential ψ_0, the Poisson−Boltzmann-like eq 10 is then solved simultaneously and self-consistently with eqs 42 and 43, with the molar density of coions given by

$$[c_-] = [c_+] - [ct] = n_{NaOH} + n_{NaCl} + n_{dCAT1I} + [H^+]\left(1 + K_H[ct]\frac{e^{-\psi_0}}{\langle e^{-\psi}\rangle}\right), \quad (44)$$

and eqs 11 and 12 are evaluated with the replacements $n_\pm \rightarrow [c_\pm]$.

The experiments were performed at a temperature of $T = 25$ °C (298.15 K), at which the measured dielectric constant of the water is $\epsilon = 78.38$,[25] which leads to a Bjerrum length of $l_B = 7.15$ Å. By using an estimate of 60 Å^2 for the area of the polar headgroup, a bilayer thickness of $t = 50$ Å, and monodisperse vesicles of radius $r_0 - t/2$

(25) Archer, D. G.; Wang, P. *J. Phys. Chem. Ref. Data* **1990**, *19*, 371. These values of the water dielectric constant were obtained at the pressure $p = 0.1$ MPa.

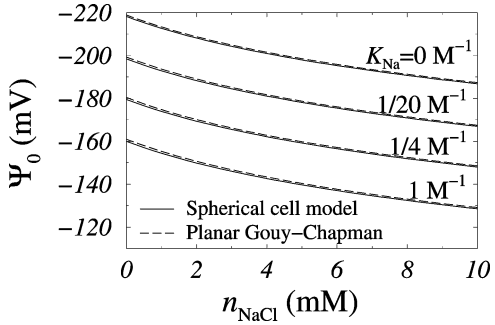

Figure 3. Comparison between theoretical predictions for the ionic-strength dependence of the surface electrostatic potential of charged vesicles. The solid lines correspond to the spherical cell model, whereas the dashed lines correspond to the planar Gouy−Chapman approximation. At this relatively dilute experimental concentration ($n_{NaPG} = 10$ mM), the two approaches give essentially the same results. The different profiles correspond to several values of the association constant K_{Na}. The calculations included the ionic-strength contribution due to the aqueous soluble cationic spin labels ($n_{dCAT1I} = 0.1$ mM), but their specific binding to the phosphate surface groups was neglected ($K_{dCAT1} = 0$ M^{-1}).

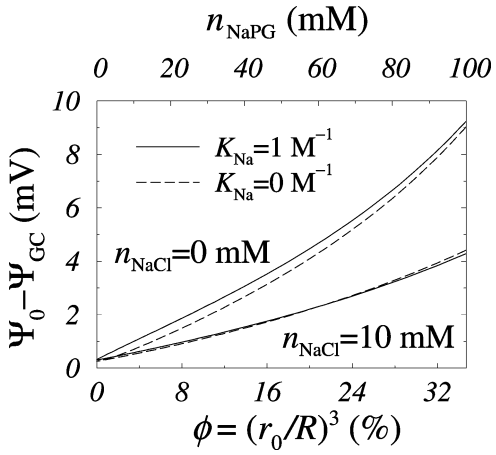

Figure 4. Dependence of the surface electrostatic potential on the vesicle concentration, measured by the volume fraction of the vesicles, $\phi = (r_0/R)^3$, or by the phospholipid concentration n_{NaPG} (converted assuming that the radius of the vesicle remains constant at $r_0 = 525$ Å). The calculations included the ionic-strength contribution due to the cationic spin labels ($n_{dCAT1I} = 0.1$ mM) but with no specific binding ($K_{dCAT1} = 0$ M^{-1}). To allow a better view, the results are presented in terms of the difference between the spherical cell model and the planar Gouy−Chapman predictions, the numerical values of which are given in Table 1. One should note, however, that the deviations are proportionally small (less than 5% of the absolute value of the surface electrostatic potential), even for concentrated suspensions.

$= 500$ Å, we estimate that the radius of the spherical cell is $R = 1610$ Å and the bare external valence is $Z_{max} = 5.77 \times 10^4$ for the DMPG concentration $n_{NaPG} = 10$ mM.[6] In the experiments, the pH was stabilized by using a 10 mM 4-(2-hydroxyethyl)-1-piperizineethanesulfonic acid (Hepes) buffer solution, p$K_A = 7.48$ at $T = 25$ °C,[26] with the pH adjusted with 4 mM of the strong base NaOH. The ionic strength was varied by adding monovalent salt (NaCl) until a concentration of $n_{NaCl} = 10$ mM was reached. The value of the proton association constant to the phosphate groups, $K_H = 15.8$ M^{-1}, was taken from the literature.[27,28]

Assuming the presence of 0.1 mM of the spin label, but no specific binding to surface phosphate groups ($K_{dCAT1} = 0$ M^{-1}) we present in Figure 3 the ionic-strength dependence of the electrostatic potential for $n_{NaPG} = 10$ mM and some values of K_{Na} in the range of [0, 1] M^{-1} within the spherical cell model. For comparison, we also show results within the planar-symmetry Gouy−Chapman approximation (cf. Appendix B). It can be seen from the figure that the two approaches give essentially the same results for the surface electrostatic potential at this lipid concentration. However, this is true only when the vesicle density is sufficiently low.

Deviations from the planar results can be observed at higher lipid concentrations. In Figure 4, we show the dependence of the surface electrostatic potential on the lipid concentration for several fixed values of the association constant K_{Na} and the added monovalent salt concentration n_{NaCl}. The results are presented in terms of the difference between the spherical cell model and the planar Gouy−Chapman predictions. The dependence of the surface electrostatic potential with the vesicle concentration is enhanced as the ionic strength is lowered. Note, however, that the finite-density, spherical-symmetry effects are not very drastic because the deviations are proportionally small (less than 5% of the absolute value of the surface electrostatic potential), even for concentrated suspensions.

In fact, we can observe that the surface potentials obtained under the planar-symmetry Gouy−Chapman model (cf. Appendix B) represent an upper bound for the values in spherical symmetry for finite densities of vesicles. The infinite-dilution limit of Ψ_0 is very close to the Gouy−Chapman value, although not rigorously exact. The agreement is, however, asymptotically exact[29,30] in the limit of strong screening, $\kappa r_0 \to \infty$.

For the conditions of the reported experiments in this subsection—in which the concentrations of the protons (pH ≈ 7.4) and the cationic spin labels ($n_{dCAT1I} = 0.1$ mM) are much smaller than the density of the sodium cations—the surface charge density and electrostatic potential are quite insensitive to variations in the association constants K_H and K_{dCAT1} (not shown). However, this independence *does not* apply to the partition ratios of the cationic species, which is considered in the next subsection.

B. Partition Ratios for the Cationic Spin Labels. For the dispersion of DMPG unilamellar vesicles, the partition ratio (eq 40) of the aqueous soluble cationic spin labels can be rewritten as

$$P = \frac{1}{(v_{eff} + v_{int})n_{dCAT1I}}\left(v_{int}n_{dCAT1I} + v_{eff}[dCAT1PG_{surf}] + \frac{4\pi r_0^{\,3}}{\langle e^{-\psi}\rangle}[dCAT1^+]\int_1^{\bar{\xi}} d\xi\, \xi^2 e^{-\psi(\xi)}\right)$$

$$= \frac{1}{1 + \phi[(1-\tau)^3 - 1]}\left[\phi(1-\tau)^3 + \frac{1-\phi}{e^{\psi_0}\langle e^{-\psi}\rangle + K_{dCAT1}[ct]}\left(K_{dCAT1}[ct] + \frac{3\phi e^{\psi_0}}{1-\phi}\int_1^{\bar{\xi}} d\xi\, \xi^2 e^{-\psi(\xi)}\right)\right], \quad (45)$$

in which $\tau = t/r_0$ is the ratio between the bilayer thickness

(26) Good, N. E.; Winget, G. D.; Winter, W.; Connolly, T. N.; Izawa, S.; Singh, R. M. M. *Biochemistry* **1966**, *5*, 467. This work determines the Hepes pK_A($T = 20$ °C) = 7.55 with ΔpK_A/°C = −0.014.

(27) Watts, A.; Harlos, K.; Maschke, W.; Marsch, D. *Biochim. Biophys. Acta* **1978**, *510*, 63.

(28) Toko, K.; Yamafuji, K. *Chem. Phys. Lipids* **1980**, *26*, 79.

(29) Ramanathan, G. V. *J. Chem. Phys.* **1988**, *88*, 3887.

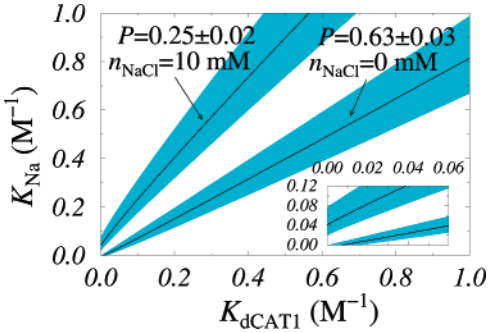

Figure 5. Values of the spin label and sodium cations association constants to the phosphate surface groups K_{dCAT1} and K_{Na}, which yield the experimentally measured partition ratios for the lowest ($n_{NaCl} = 0$ mM) and highest ($n_{NaCl} = 10$ mM) ionic strengths. The shaded regions represent the effect of the error bars of the experimentally measured partition ratios on the theoretical prediction (solid lines). The concentrations of the phospholipid DMPG ($n_{NaPG} = 10$ mM) and of the spin labels ($n_{dCAT1I} = 0.1$ mM) were kept constant. The range of variation of the association constant K_{Na} is reduced as the value of K_{dCAT1} decreases. However, it is not possible apparently to obtain unique values of K_{Na} and K_{dCAT1} that cover the whole range of ionic strengths. The inset shows the behavior of the two curves close to the origin.

t and the vesicle radius r_0, and $\phi = (r_0/R)^3$ is the volume fraction occupied by the vesicles in the suspension. The bound probes include, in addition to the electrostatically associated probes, those probes specifically adsorbed to phosphate surface groups, which give rise to the surface density $\sigma_{dCAT1PG} = v_{eff}[dCAT1PG_{surf}]/(4\pi r_0^2)$, and those located in the aqueous compartment of volume $v_{int} = (4\pi/3)(r_0 - t)^3$ surrounded by the bilayer. The latter probes were included because the probability density $\xi^2 e^{-\psi(\xi)}$ is a monotonic increasing function in the interior of the vesicle ($0 \le \xi \le 1 - \tau$).

Contrary to the surface charge density and the electrostatic surface potential, which were investigated in the previous subsection, the partition ratios of the cationic species are quite sensitive to the value of the association constants. However, no direct measurements of the association constants nor of the surface charge density of the vesicles were reported. The only available experimental measurements for the described experiments[12] are the spin-label partition ratios. Thus, to compare the experimental partition ratios with the theoretical predictions given by eq 45, which are calculated using the model described in subsection IV-A and developed throughout the manuscript, one has to, therefore, attribute values to the association constants for sodium cations K_{Na} and for the cationic probe K_{dCAT1} to the phosphate surface groups. Figure 5 shows the calculated values of these two association constants, such that the experimentally measured partition ratio[12] equals the theoretical prediction, given by eq 45. To estimate the effect of the error bars of the experimentally measured partition ratios on the values of the dissociation constants, we also plotted in Figure 5 the predicted range of these constants within the experimental error bars. Furthermore, we also considered the effect of the lack of accuracy in the determination of the vesicle radius. By using an estimate between 400 and 500 Å, we obtained the intercepts of the curves and the axes in Figure 5 for the lowest and highest salt concentrations. The obtained results are quite insensitive to the variation of the vesicle radius: $K_{dCAT1} = (0.0072 \pm 0.0002)$ M^{-1} for $K_{Na} = 0$ M^{-1}, $P = 0.63$, and $n_{NaCl} = 0$ mM (lowest ionic strength); and $K_{Na} = (0.043 \pm 0.003)$ M^{-1} for $K_{dCAT1} = 0$ M^{-1}, $P = 0.25$, and $n_{NaCl} = 10$ mM (highest ionic strength). Therefore, the conclusions below remain unaltered, even if the radii of the vesicles vary by as much as 20%. The most relevant contribution to the error arises from the experimental error bars of the partition ratios and not from the uncertainty in the determination of the radius of the vesicles. Several conclusions can be drawn from Figure 5. For salt-free suspensions, a bilayer that has a proton association $K_H \neq 0$ M^{-1} with no further cationic association ($K_{dCAT1} \approx K_{Na} \approx 0$ M^{-1}) is *marginally* consistent with the salt-free experimentally measured partition ratios. In general, however, it is not possible to reproduce the salt-free experimental data by assuming that there is no specific binding of the cationic spin labels ($K_{dCAT1} = 0$ M^{-1}). A finite association constant for sodium K_{Na} is also required, at least for higher salt concentrations. Full calculation of the electrostatic potential requires additional information from experimental measurements.

The previous study, which was based on the Gouy–Chapman model for an infinite charged plane in contact with a monovalent salt reservoir and null specific binding of the probe ($K_{dCAT1} = 0$ M^{-1}), pointed to a variation in the sodium association constant K_{Na} with ionic strength. The range of variation of K_{Na} obtained by this simplified model[12] was predicted to be 0.17–0.84 M^{-1} for $n_{dCAT1I} = 0.1$ mM. These predicted values lie within the range reported in the literature (e.g., see ref 6 and the references therein), but are in contradiction with our theoretical predictions for $K_{dCAT1} = 0$ M^{-1}. According to our calculations shown in Figure 5, to obtain this previously predicted range of variation for K_{Na}, one should instead have a nonvanishing association constant for the cationic probe K_{dCAT1} in the range of 0.23–0.47 M^{-1}. The crucial difference between the two approaches lies in the definition of the partition ratios. In our calculation, the existence of the geometric factor r^2 in the probability density to find a positive microion at the position r is fundamental (cf. eq 39). It is this geometric factor that allows us to define the radius $\bar{r}$, below which the cationic species are classified as bound. In the simplified model of ref 12, the partition ratio was instead estimated using a box model with two homogeneous concentrations and an arbitrary thickness h of the region where the bound probes reside, which plays the role of $\bar{\xi}$ in our treatment (cf. eq 39).

Use of a different monovalent salt (e.g., KCl) induces changes in the light-scattering profile compared to NaCl,[31] suggesting that there is indeed a specific binding of cations to the vesicle surface. It would be interesting if the conclusions drawn from this model were backed up by direct measurements of the vesicle surface charge.

V. Conclusions

We have developed a general approach for the calculation of the electrostatic potential for aqueous suspensions of charged spherical colloids in the presence of monovalent salts and buffer. Accounting for the spherical geometry and the finite colloid concentration requires much more involved calculations. We have shown that, for dilute suspensions, both geometries—planar and spherical—yield very similar results, and therefore, in the case of dilute systems, it is appropriate to consider the much simpler planar geometry. However, away from the dilute regime, the correct geometry must be considered because, as we also show, the difference with respect to the planar approximation increases both with increasing colloid concentration and decreasing ionic strength.

(30) Shkel, I. A.; Tsodikov, O. V.; Record, M. T., Jr. *J. Phys. Chem. B* **2000**, *104*, 5161.

(31) Riske, K. A. M.S. Thesis, University of São Paulo, Brazil, 1997.

Although in this work we treated only ionogenic surfaces containing ionizable monovalent acidic groups, our method can be extended to include different types of surface chemistry. For example, we did not treat amphoretic surfaces[32,33] in which the same *neutral* surface group HA may either dissociate to yield a proton to the solution ($HA_{surf} \rightleftharpoons H^+ + A^-_{surf}$) or take up a proton from the solution ($HA_{surf} + H^+ \rightleftharpoons H_2A^+_{surf}$). Furthermore, we also do not consider zwitterionic surfaces (common in biological systems) containing both basic (e.g., amino) and acidic (e.g., carboxyl) groups (one capable of accepting a proton and one capable of dissociating to release a proton) nor surfaces that possess two distinct acid dissociation sites (e.g., latex colloids containing sulfonic or sulfate (strong acid) and carboxylic (weak acid) groups). This latter class of systems was considered in ref 34 with the proton concentration $[H^+]$ adjusted by balancing known amounts of strong acid and strong base. All of these classes of systems can also be considered when performing suitable changes in the equations governing the surface charge regulation.

We also propose a procedure for calculating the partition ratio of specific ions, which allows for the possibility of specific binding in two different environments: near the charged surface and in the aqueous solution. Comparison of our approach with experimental data for aqueous DMPG suspensions indicates the need to take into account the specific adsorption of the cationic probe and, in general, that of any cationic species present in solution to the phosphate surface groups. Despite the similarity between the results derived from both geometries, note that additional experimental data is needed to allow for the prediction of the surface electrostatic potential.

Despite some effort,[7−11] the peculiar thermotropic behavior of aqueous DMPG suspensions has not been fully explained, particularly with respect to electrical properties, such as conductivity. It has been shown[6] that conductivity rises around the region of low scattering of light. On the other hand, our study points to an enhancement of K_{Na} with ionic strength at a fixed temperature. An inspection of the scattering versus temperature plots for different ionic strengths[12] shows that increasing ionic strength at a fixed temperature requires leaving the pseudophase associated with low scattering of light. One might conjecture that the decrease in the reduced conductivity, defined as the difference between the measured conductivity and the conductivity due to the added electrolyte only, is a consequence of an increment in K_{Na}. In any case, this approach must certainly contribute to clarify the relevance of charge effects on the thermal behavior of the lipid dispersion. However, an attempt to relate these changes to the different phases observed experimentally would require looking into chain transitions and their effect on colloid geometry, particularly on the colloid radius. A different approach would be needed to include the electrostatic treatment in theories based on colloid elasticity or the thermodynamics of the dispersion.

Acknowledgment. This work was supported by the University of São Paulo (USP) and Fundação de Amparo à Pesquisa do Estado de São Paulo (FAPESP). Fellowships for M.N.T. (post-doctor, FAPESP) and M.T.L. (research, CNPq − Conselho Nacional de Desenvolvimento Cientıfico e Tecnológico) are acknowledged. The authors also thank Carla Goldman for fruitful discussions.

Appendix A: Buffer Solution

In this appendix, we present the standard treatment of a buffer solution as a homogeneous electrolyte, neglecting activity coefficients and the presence of the charged colloids.

A buffer is an aqueous solution of a weak acid (HA) of initial total concentration (before ionization) n_{HA} counterbalanced by a strong base of concentration n_{XOH}, which undergoes complete ionization in water ($XOH \rightarrow X^+ + OH^-$), thus implying that $[X^+] = n_{XOH}$. The equilibrium constants (neglecting activity coefficients) associated to the water autoprotolysis ($H_2O \rightleftharpoons H^+ + OH^-$) and the reversible partial ionization of the weak acid ($HA \rightleftharpoons H^+ + A^-$) read

$$K_W = [H^+][OH^-], \tag{A1}$$

$$K_A = \frac{[H^+][A^-]}{[HA]} = \frac{[H^+][A^-]}{n_{HA} - [A^-]}. \tag{A2}$$

At $T = 25$ °C, the ionic product of the water assumes the numerical value $pK_W = -\log K_W = 13.995$,[35] in which the symbol log denotes the decimal logarithm. The overall electroneutrality of the buffer solution implies that $[H^+] = [OH^-] + [A^-] - [X^+] = K_W/[H^+] + n_{HA}/(1 + [H^+]/K_A) - n_{XOH}$, yielding a cubic equation for $[H^+]$,

$$K_W K_A = [H^+]^3 + (K_A + n_{XOH})[H^+]^2 - \{K_W + K_A(n_{HA} - n_{XOH})\}[H^+]. \tag{A3}$$

To adjust the pH ($= -\log[H^+]$) of a 10 mM Hepes buffer solution to ~7.4 at $T = 20$ °C, 4 mM of the strong base NaOH is added. Using the Hepes $pK_A = -\log[K_A] = 7.55$ (standardized at $T = 20$ °C)[26] and the ionic product of the water ($pK_W = 14.163$),[35] we obtain the theoretical value $pH = -\log[H^+] = 7.374$, which is close enough to the experimentally measured value of pH = 7.4. Because the buffer solution pH and the added base concentration n_{NaOH} can be measured simultaneously, this represents an experimental confirmation of the standard value of the Hepes pK_A. However, the pH adjustment at $T = 20$ °C is shifted as the temperature changes. For example, for experiments performed at $T = 25$ °C, using the standardized values $pK_A = 7.48$,[26] and $pK_W = 13.995$,[35] we obtain the theoretical prediction pH = 7.304 for the same amount of the added base ($n_{NaOH} = 4$ mM).

In the limit $n_{XOH} \gg [H^+]$ and $n_{XOH} \gg [OH^-]$, the solution to eq A3 can be approximated by taking $[A^-] \approx n_{XOH}$ in the Henderson−Hasselbalch equation,[36] which results from the eq A2 that defines K_A,

$$pH = pK_A + \log\left(\frac{[A^-]}{n_{HA} - [A^-]}\right) \approx pK_A + \log\left(\frac{n_{XOH}}{n_{HA} - n_{XOH}}\right), \tag{A4}$$

or $n_{XOH} \approx n_{HA}/(1 + 10^{pK_A - pH})$.

(32) Campos, A. F. C.; Tourinho, F. A.; da Silva, G. J.; Lara, M. C. F. L.; Depeyrot, J. *Eur. Phys. J. E* **2001**, *6*, 29.
(33) Tourinho, F. A.; Campos, A. F. C.; Aquino, R.; Lara, M. C. F. L.; da Silva, G. J.; Depeyrot, J. *Braz. J. Phys.* **2002**, *32*, 501.
(34) Gisler, T.; Schulz, S. F.; Borkovec, M.; Sticher, H.; Schurtenberger, P.; D'Aguanno, B.; Klein, R. *J. Chem. Phys.* **1994**, *101*, 9924.
(35) Lide, D. R., Ed. *CRC Handbook of Chemistry and Physics*, 78th ed.; CRC Press: Boca Raton, 1997; pp 6−8 and 8−80. Values of $pK_W(T)$ at saturated vapor pressure: $pK_W(T = 20\ °C, p = 2.3388\ kPa) = 14.163$; $pK_W(T = 25\ °C, p = 3.1690\ kPa) = 13.995$; $pK_W(T = 30\ °C, p = 4.2455\ kPa) = 13.836$.

During investigations of the effect of H^+ ions on the activity of enzymes, Sørensen[37] introduced in 1909 the term $pH = -\log[H^+]$. Later he realized, however, that the pH of a solution is determined by the activity of the H^+ ion (not just by its molar concentration, $[H^+]$), and, in 1924, published a second paper on the subject,[38] defining $pH \equiv -\log a_{H^+}$, in which $a_{H^+} = \gamma_+[H^+]$ denotes the activity of the H^+ ion in terms of the activity coefficient γ_+. The question is more troublesome than it may look because single-ion activities are immeasurable quantities. Therefore, pH can only be measured relative to other solutions in which pH has been defined in some arbitrary way. For this purpose, accurate pH measurements have been standardized by the International Union of Pure and Applied Chemistry (IUPAC), a subject that is still under development.[39−41]

In the above theoretical analysis, we neglected the ionic-strength dependence of the equilibrium constants by setting the ionic activity coefficients to one. Therefore, under this approximation, the above analysis remains unchanged with the addition of the monovalent salt NaCl and the iodide salt corresponding to the aqueous soluble spin label dCAT1I. However, if we were to use the Debye−Hückel limiting expressions for the activity coefficients of the charged species,[42] a small correction of $\Delta pH \approx -0.06$ would be obtained for the highest employed ionic strength, $n \approx 14$ mM.

Appendix B: Gouy−Chapman Model with Charge Regulation

In ref 12, in addition to the planar geometry, the high-potential approximation was used to estimate the surface potential in the framework of the Gouy−Chapman model. In this appendix, we consider the Gouy−Chapman equations without any further approximations.

The analytical solution of the one-dimensional version of the Poisson−Boltzmann equation

$$\frac{d^2\psi(r)}{dr} = \kappa^2 \sinh \psi(r), \tag{B1}$$

in which $\kappa \equiv \sqrt{8\pi l_B 10^3 N_A n}$ is the inverse Debye screening length, and $n = [H^+] + n_{NaOH} + n_{NaCl} + n_{dCAT1I}$ is the bulk ionic strength (due to protons, sodium cations, and cationic spin labels), leads to the boundary condition for the dimensionless surface electrostatic potential ψ_0,

$$\sinh \frac{\psi_0}{2} = -\frac{\alpha}{\kappa\Lambda}, \tag{B2}$$

in which $\Lambda = 1/(2\pi l_B \sigma_{max})$ is the Gouy−Chapman length[21,43,44] associated with the bare surface charge density $\sigma_{max} = Z_{max}/(4\pi r_0^2)$, and α is the fraction of actually ionized sites on the charged plane,

$$\alpha = \frac{[PG^-_{surf}]}{[PG^-_{surf}] + [HPG_{surf}] + [NaPG_{surf}] + [dCAT1PG_{surf}]} = \frac{1}{1 + K_H[H^+]_{r_0} + K_{Na}[Na^+]_{r_0} + K_{dCAT1}[dCAT1^+]_{r_0}} = \frac{1}{1 + \eta e^{-\psi_0}}, \tag{B3}$$

in which $\eta \equiv K_H[H^+] + (n_{NaOH} + n_{NaCl})K_{Na} + n_{dCAT1I}K_{dCAT1}$, and all of the concentrations are measured in the bulk, where the electrostatic potential is set to zero ($\psi \equiv 0$). The bulk proton concentration $[H^+]$ is given by the solution of the cubic eq A3 with $n_{XOH} = n_{NaOH}$, which can be approximated by $[H^+] \approx K_A(n_{HA} - n_{NaOH})/n_{NaOH}$. By combining eqs B2 and B3, we obtain a fourth-order equation for $e^{-\psi_0/2}$,

$$\eta e^{-2\psi_0} + (1 - \eta)e^{-\psi_0} - \frac{2e^{-\psi_0/2}}{\kappa\Lambda} - 1 = 0, \tag{B4}$$

the real solution of which gives the surface electrostatic potential in the Gouy−Chapman approximation $\Psi_{GC} \equiv \psi_0/(\beta q)$ used to plot Figure 4.

An asymptotic formula (for $\kappa r_0 \to \infty$) of the electrostatic surface potential for spherical symmetry was proposed by Loeb et al.,[45]

$$\sinh \frac{\psi_0}{2} + \frac{2}{\kappa r_0} \tanh \frac{\psi_0}{4} = -\frac{\alpha}{\kappa\Lambda}, \tag{B5}$$

which leads to an algebraic equation for $e^{-\psi_0/2}$,

$$\left[\eta e^{-2\psi_0} + (1 - \eta)e^{-\psi_0} - \frac{2e^{-\psi_0/2}}{\kappa\Lambda} - 1\right](1 + e^{-\psi_0/2}) = \frac{4e^{-\psi_0/2}}{\kappa r_0}(1 - e^{-\psi_0/2})(1 + \eta e^{-\psi_0}), \tag{B6}$$

which can be compared with the exact solutions in the planar and spherical symmetries. For the conditions of the reported experiments in subsection IV-A, the difference

Table 1. Comparison between the Theoretical Predictions for the Surface Electrostatic Potential (given in mV) Obtained under the Planar-Symmetry Gouy−Chapman Approximation (Eq B4) and by Using Loeb's Asymptotic Formula for Spherical Symmetry (Eq B6)[a]

K_{Na}	$n_{NaCl} = 0$ mM	$n_{NaCl} = 10$ mM
	Gouy−Chapman	
1 M^{-1}	−160.98	−129.09
0 M^{-1}	−218.92	−187.35
	Loeb et al.	
1 M^{-1}	−160.67	−128.80
0 M^{-1}	−218.67	−187.11

[a] The parameters used to perform the calculations correspond to the conditions of the reported experiments of subsection IV-A. As can be seen from the numerical values, under these conditions, the difference between the two approximations is a fraction of mV.

(36) Atkins, P. W. *Physical Chemistry*, 6th ed.; Oxford University Press: Oxford, 2000; Section 9.5.
(37) Sørensen, S. P. L. *Biochem. Z.* **1909**, *21*, 131.
(38) Sørensen, S. P. L.; Linderstrøm-Lang, K. L. *C. R. Trav. Lab. Carlsberg* **1924**, *15*, 1.
(39) Buck, R. P.; Rodinini, S.; Covington, A. K.; Baucke, F. G. K.; Brett, C. M. A.; Camões, M. F.; Milton, M. J. T.; Mussini, T.; Naumann, R.; Pratt, K. W.; Spitzer, P.; Wilson, G. S. *Pure Appl. Chem.* **2002**, *74*, 2169.
(40) Baucke, F. G. K. *Anal. Bioanal. Chem.* **2002**, *374*, 772.
(41) Spitzer, P.; Werner, B. *Anal. Bioanal. Chem.* **2002**, *374*, 787.
(42) McQuarrie, D. A. *Statistical Mechanics*; University Science Books: Sausalito, CA, 2000; Chapter 15. Debye−Hückel mean activity coefficient: $\gamma = (\gamma_+^{\nu_+}\gamma_-^{\nu_-})^{1/(\nu_+ + \nu_-)}$ for the salt dissociation $X_{\nu_+}Y_{\nu_-} \to \nu_+X^+ + \nu_-Y^-$ is given by $\ln \gamma = -|z_+z_-|\kappa l_B/2$, in which $\kappa = \sqrt{8\pi l_B 10^3 N_A n}$; $n = (1/2)(z_+^2 n_+ + z_-^2 n_-)$.
(43) Gouy, G. *J. Phys. Paris* **1910**, *9*, 457; *Ann. Phys.* **1917**, *7*, 129.
(44) Chapman, D. L. *Philos. Mag.* **1913**, *25*, 475.
(45) Loeb, A. L.; Wiersema, P. H.; Overbeek, J. Th. G. *The Electrical Double Layer Around a Spherical Colloid Particle*; MIT Press: Cambridge, MA, 1961.

between the surface electrostatic potential obtained under the planar-symmetry Gouy−Chapman approximation (eq B4) and that obtained by using Loeb's asymptotic formula for spherical symmetry (eq B6) is a fraction of mV (cf. Table 1).

LA051211Q